Biomech Model Mechanobiol (2013) 12:417–429
DOI 10.1007/s10237-012-0409-4

ORIGINAL PAPER

The effect of collagen degradation on chondrocyte volume and morphology in bovine articular cartilage following a hypotonic challenge

S. M. Turunen · M. J. Lammi · S. Saarakkala · S.-K. Han · W. Herzog · P. Tanska · R. K. Korhonen

Received: 17 November 2011 / Accepted: 22 May 2012 / Published online: 19 June 2012
© Springer-Verlag 2012

Abstract Collagen degradation is one of the early signs of osteoarthritis. It is not known how collagen degradation affects chondrocyte volume and morphology. Thus, the aim of this study was to investigate the effect of enzymatically induced collagen degradation on cell volume and shape changes in articular cartilage after a hypotonic challenge. Confocal laser scanning microscopy was used for imaging superficial zone chondrocytes in intact and degraded cartilage exposed to a hypotonic challenge. Fourier transform infrared microspectroscopy, polarized light microscopy, and mechanical testing were used to quantify differences in proteoglycan and collagen content, collagen orientation, and biomechanical properties, respectively, between the intact and degraded cartilage. Collagen content decreased and collagen orientation angle increased significantly ($p < 0.05$) in the superficial zone cartilage after collagenase treatment, and the instantaneous modulus of the samples was reduced significantly ($p < 0.05$). Normalized cell volume and height 20 min after the osmotic challenge (with respect to the original volume and height) were significantly ($p < 0.001$ and $p < 0.01$, respectively) larger in the intact compared to the degraded cartilage. These findings suggest that the mechanical environment of chondrocytes, specifically collagen content and orientation, affects cell volume and shape changes in the superficial zone articular cartilage when exposed to osmotic loading. This emphasizes the role of collagen in modulating cartilage mechanobiology in diseased tissue.

Keywords Articular cartilage · Mechanobiology · Microscopy · Enzymatic treatment · Collagen · Chondrocytes

S. M. Turunen (✉) · S. Saarakkala · P. Tanska · R. K. Korhonen
Department of Applied Physics, University of Eastern Finland, POB 1627, 70211 Kuopio, Finland
e-mail: siru.turunen@uef.fi

M. J. Lammi
Department of Biomedicine, University of Eastern Finland, POB 1627, 70211 Kuopio, Finland

M. J. Lammi
Biocenter Kuopio, University of Eastern Finland, POB 1627, 70211 Kuopio, Finland

S. Saarakkala
Department of Diagnostic Radiology, University of Oulu and Oulu University Hospital, Oulu, Finland

S.-K. Han · W. Herzog
Human Performance Laboratory, Faculty of Kinesiology, University of Calgary, Calgary, AB, Canada

S.-K. Han · W. Herzog
Mechanical and Manufacturing Engineering, Schulich School of Engineering, University of Calgary, Calgary, AB, Canada

S.-K. Han
Fischell Department of Bioengineering, Clark School of Engineering, University of Maryland, Maryland, USA

1 Introduction

Articular cartilage is comprised of cells (chondrocytes, ~1–10 % of the volume fraction) that are embedded in an extracellular matrix (ECM) consisting of proteoglycans (PGs, 4–7 % of the wet weight), collagen (10–20 % of the wet weight), and interstitial fluid (65–80 % of the wet weight) (e.g., Mankin et al. 1994; Stockwell and Meachim 1973; Stockwell 1991). The structure of articular cartilage shows a zonal variation throughout the tissue depth (Stockwell and Meachim 1973; Mankin et al. 1994). Specifically, cells in the superficial zone are oval, flattened, and surrounded by the tangentially oriented collagen fibers, while the PG content is in its lowest and fluid fraction in its highest level in this zone.

The chondrocyte and the surrounding pericellular matrix (PCM) form the chondron (Poole 1997). The PCM contains more PGs than the ECM, and the primary connection from the PCM to the ECM and chondrocyte is through type VI collagen fibrils (Poole et al. 1992). Chondrocytes maintain the integrity of the ECM and PCM by producing PGs and collagen (Stockwell 1991), while the PCM has been suggested to mechanically protect cells (Guilak et al. 2006; Poole et al. 1988). Together with the ECM, the PCM has also been suggested to modulate biomechanical and biophysical signals perceived by chondrocytes and, consequently, cartilage mechanotransduction (Alexopoulos et al. 2005; Guilak et al. 2006; Guilak 2011; Millward-Sadler and Salter 2004).

The extracellular osmolarity in healthy articular cartilage is around 350–480 mOsm, depending on the cartilage composition and zone (Urban et al. 1993). Osteoarthritis (OA) is characterized by structural and compositional changes in the collagen network, reduced PG content, and an increased fluid fraction (Arokoski et al. 2000; Grushko et al. 1989; Maroudas and Venn 1977; Stockwell 1991). These alterations in cartilage composition have been shown to lead to reduced extracellular osmolarity and increased chondrocyte volume (Bush and Hall 2003; Urban et al. 1993). Altered chondrocyte volume may result in altered cell biosynthesis (Buschmann et al. 1996; Newman and Watt 1988; Urban et al. 1993) and mechanotransduction (Buschmann et al. 1996), affecting also OA progression.

Several previous studies have investigated the relationships between ECM and PCM properties and chondrocyte volume and morphology in osmotically challenged cartilage. Hing et al. (2002) showed that size and structure of the PCM modulate chondrocyte response to osmotic challenge. Korhonen et al. (2010a,b) suggested that chondrocyte shapes in hypo-osmotically challenged rabbit articular cartilage are modulated along the primary collagen fibril directions. A recent study (Korhonen et al. 2011) showed that especially the progressive collagen loss of the PCM and ECM in the superficial tissue of spontaneously degenerated human articular cartilage modulates cell morphology during the progression of OA. Furthermore, Turunen et al. (2012) suggested that the integrity of the mechanical environment of chondrocytes affects superficial zone cell volume and shape changes following the hypotonic challenge of bovine cartilage. Although these aforementioned studies suggest that the ECM and PCM, especially the collagen network, modulate cell function, it has not been directly shown how different constituents of the ECM affect cell volume and morphology in osmotically challenged articular cartilage.

Cell volumes in the superficial zone of intact cartilage (measurements taken through the intact cartilage surface) have been found to be significantly larger at steady state after a hypotonic challenge (from tens of minutes to several hours) than before the challenge (Korhonen et al. 2010b; Turunen et al. 2012), while they have been found to recover to the original volume in explant tissues (measurements conducted through the cut surface) (Bush and Hall 2001a; Turunen et al. 2012). Isolated cells have been found to follow the behavior of cells in explant tissues (Bush and Hall 2001a). These differences in cell mechanics between intact and explant tissues/isolated chondrocytes may be related to the integrity of the collagen network and collagen content. However, this relationship has yet to be explored.

Using OA cartilage, it is impossible to separate the effects of different cartilage constituents on cell responses. In order to study specifically the effect of collagen fibril degradation on biomechanical, biochemical, and organizational changes in articular cartilage, enzymatic treatment using collagenase has been used to selectively digest the collagen fibril network (Kikuchi et al. 1998; Korhonen et al. 2003; Långsjö et al. 2002; Lyyra et al. 1999; Nieminen et al. 2000; Rieppo et al. 2003; Töyräs et al. 1999). Previous studies have shown that collagenase treatment reduces superficial collagen fibril diameter and collagen network stiffness (Table 1), and increases collagen content in the incubation medium (Korhonen et al. 2003; Långsjö et al. 2002; Rieppo et al. 2003). Also birefringence, an estimate of the collagen fibril organization and quantity (Arokoski et al. 1996) has been shown to decrease significantly in the superficial zone of cartilage after collagenase treatment (Table 1) (Rieppo et al. 2003), suggesting more isotropic collagen fibril orientation (more random collagen orientation) in the degraded than the intact cartilage. Several experimental techniques have been used in these earlier studies to characterize the changes in the properties of cartilage following collagen degradation, such as transmission electron microscopy (TEM), polarized light microscopy (PLM), biochemical methods, and biomechanical tests (Korhonen et al. 2003; Långsjö et al. 2002; Rieppo et al. 2003). However, there is no experimental data on how degradation of the collagen network, as characterized with the above-mentioned techniques, may affect cell volume and morphology in articular cartilage exposed to hypotonic challenges.

As stated above, OA induces changes in the extracellular osmolarity, ECM structure, and cell volume, which may alter cartilage biosynthesis. However, it is not known how collagen composition and organization affect cell volume in osmotically challenged cartilage. In order to determine the specific role of collagen degradation on cell volume and morphology, we investigated the intact and enzymatically degraded (collagen degradation) bovine articular cartilage. Superficial zone chondrocytes in intact and degraded cartilage were imaged before and at steady state after a hypotonic challenge using confocal laser scanning microscopy (CLSM). Changes in cartilage composition, collagen architecture, and biomechanical properties of intact and degraded cartilage were quantified with Fourier transform infrared

Table 1 Mean values of collagen fibril diameter, birefringence, and initial and strain-dependent fibril network modulus in intact and collagenase-treated cartilage, as characterized in earlier studies (Korhonen et al. 2003; Långsjö et al. 2002; Rieppo et al. 2003). All of the parameters decreased after collagenase treatment

	Intact cartilage	Collagenase treated cartilage
Collagen fibril diameter* Långsjö et al. (2002)	38 nm	13 nm
Birefringence* Rieppo et al. (2003)	0.34×10^3	0.17×10^3
Initial fibril network modulus** Korhonen et al. (2003)	0.77 MPa	0.23 MPa
Strain-dependent fibril network modulus** Korhonen et al. (2003)	144 MPa	46 MPa

The fibril network modulus is expressed by the equation $E_f = E_f^0 + E_f^{\varepsilon}\varepsilon_f$, where E_f^0 is the initial fibril network modulus, E_f^{ε} is the strain-dependent fibril network modulus, and ε_f is tensile strain of the fibrils (Li et al. 1999; Korhonen et al. 2003)

* $p < 0.05$

** Statistics were not calculated

(FTIR) microspectroscopy, PLM, and biomechanical testing, respectively. We hypothesized that normalized cell volumes (cell volume after the challenge divided by cell volume before the challenge) at steady state after a hypotonic challenge are greater in the intact compared to the degraded cartilage. Since there is no direct experimental evidence of the role of the collagen network on changes in chondrocyte volume and morphology, the knowledge gained from this study will improve understanding of one specific mechanism that may modulate cell mechanics and mechanobiological responses of cartilage in OA.

2 Materials and methods

2.1 Preparation of isotonic and hypotonic solutions

Isotonic and hypotonic solutions were prepared using Dulbecco's modified eagle's medium (DMEM with L-glutamine, phenol red-free, low glucose, serum-free, Invitrogen, Paisley, UK) supplemented with antibiotics (100 U ml^{-1} penicillin and 100 µg ml^{-1} streptomycin, EuroClone S.p.A., Italy), and fungicide (Fungizone, Invitrogen, Paisley, UK, 2.5 µg ml^{-1}). Medium osmolarities of 285 mOsm (isotonic) and 170 mOsm (hypotonic) were prepared and controlled with a freezing-point osmometer (Halbmikro-osmometer, GWB, Knauer & Co GmbH, Berlin, Germany). Similar medium osmolarities have been used previously (Bush and Hall 2001a,b, 2005; Korhonen et al. 2010a,b). The extracellular osmolarity is affected by tissue composition (fixed charge density, water fraction, and collagen content) and osmolarity of the bathing media. Based on a study by Bush and Hall (2005), medium osmolarities used in our study create extracellular osmolarities of ~450 and ~280 mOsm. The pH was maintained at 7.4 for both solutions.

2.2 Sample preparation

Osteochondral samples from intact bovine knee joints were prepared for the experiments on the day of slaughter ($n = 7$, age 17–32 months). The samples were collected from the lateral trochlear facet using a drill bit (diameter = 21 mm) and an autopsy saw (Stryker Autopsy Saw 868, Stryker Europe BV, Uden, the Netherlands) (Fig. 1a). Two cylindrical osteochondral samples (diameter = 10 mm) were then obtained using a metallic punch. Samples were incubated for 24–48 h in isotonic DMEM at 37 °C (Turunen et al. 2012). One of the samples was used as a control (intact cartilage, $n = 7$) and the other was digested with collagenase (degraded cartilage, $n = 7$, 30 U ml^{-1}, 24 h, high-purity collagenase type VII (C0773), Sigma-Aldrich, St. Louis, MO, USA) to induce collagen degradation. The collagenase concentration was the same as used previously (Långsjö et al. 2002; Lyyra et al. 1999; Nieminen et al. 2000; Rieppo et al. 2003) (Fig. 1b). Intact and degraded cartilages from the same joint were incubated for equal periods of time. The osteochondral samples were fully immersed in the digestion medium, allowing the enzyme to penetrate into the tissue from all sides. Prior to the CLSM imaging, samples were placed in a Petri dish filled with isotonic DMEM and labeled with 5 µM calcein-AM (Invitrogen, Eugene, OR, USA) and 60 µM propidium iodide (Sigma-Aldrich) for 30 min at room temperature (Bush and Hall 2001a,b, 2003, 2005; Korhonen et al. 2010a,b). After CLSM imaging (see below), the samples were placed in a Petri dish filled with isotonic DMEM (285 mOsm) for one hour and thereafter cut in half. One half was used for biomechanical testing while the other half was prepared for the analysis of tissue composition (collagen and PG contents) and collagen orientation using FTIR microspectroscopy and PLM, respectively (Fig. 1b). Cartilage samples without bone were prepared for biomechanical testing using a razor blade and a steel punch of 3 mm in diameter (Fig. 1b). The samples were frozen immediately after the preparation in PBS (−20 °C). Prior to biomechanical and microscopical measurements, the samples were thawed slowly in a water bath (room temperature) and further processed (Fig. 1b).

2.3 Confocal laser scanning microscopy (CLSM)

Chondrocytes were imaged through the cartilage surface (Fig. 1b) using a Nikon Eclipse TE-300 microscope (Nikon Co., Japan) with an UltraVIEW confocal laser scanner (Perkin-Elmer, UK) (Turunen et al. 2012). The laser exci-

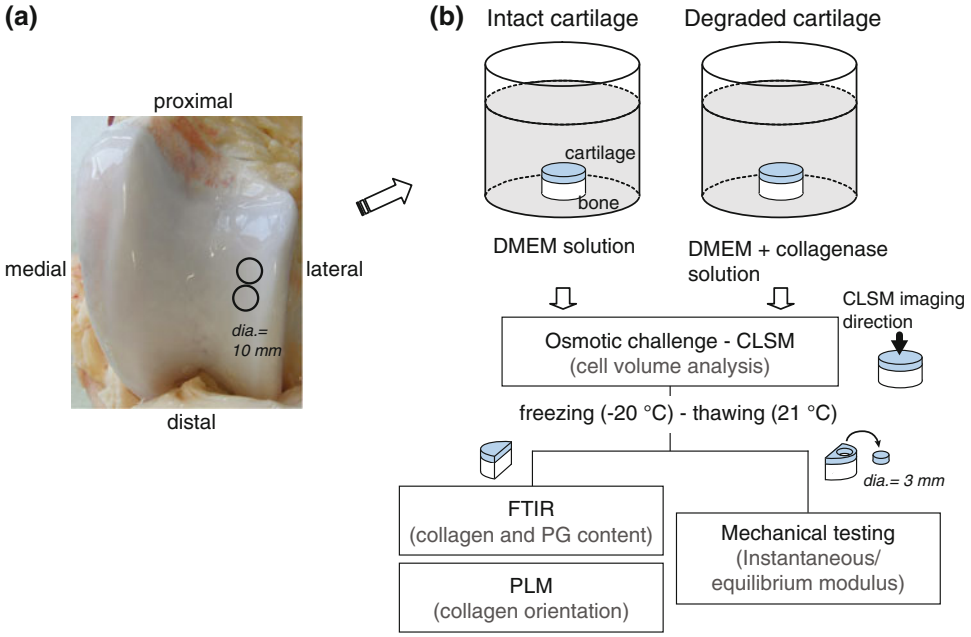

Fig. 1 Sample preparation and measurement protocol: **a** Samples were obtained from the lateral trochlear facet of bovine knee joints. **b** Adjacent samples were incubated either in DMEM or in DMEM with collagenase enzyme. Then, cell volumes in the superficial zone of intact and degraded cartilage samples were determined with confocal laser scanning microscope (CLSM) before and after an osmotic challenge. Calcein-AM-labeled chondrocytes were imaged with CLSM first in isotonic medium (285 mOsm). After this, the medium was changed to hypotonic (170 mOsm) and image stacks were captured at steady state (20 and 120 min after the osmotic challenge). Collagen and PG content, collagen orientation, and biomechanical properties of the same samples were determined with Fourier transform infrared (FTIR) microspectroscopy, polarized light microscopy (PLM), and mechanical testing

tation wavelength was 488 nm and the emitted calcein-AM fluorescence (515 nm) was measured with a band-pass filter of 500–550 nm. An objective of 60×-magnification was used.

In order to determine the resting volume of the cells before the hypotonic challenge, a reference image stack was acquired in isotonic DMEM (285 mOsm). Then, the medium was changed to hypotonic (170 mOsm) by a rapid aspiration (Korhonen et al. 2010b; Turunen et al. 2012) within ~30 s, and thereafter, image stacks were captured at steady state (20 min and 2 h). Results of some studies suggest that steady state for in situ cells is reached within 20 min (Bush and Hall 2001a), while others suggest that tissue swelling contributes to cell volume changes for hours (Korhonen et al. 2010b). Thus, 20 min and 2 h were chosen for observation. Chondrocytes up to ~60 μm from the cartilage surface were observed through the surface (Fig. 2a). Image stacks (xy-plane 672 × 512 pixels, pixel size 0.2 × 0.2 μm) were obtained with 0.26 μm vertical z-axis increments. All measurements were taken at room temperature (approximately 21 °C) (Bush and Hall 2001a,b, 2003; Korhonen et al. 2010a,b; Turunen et al. 2012).

The analysis of cell volumes has been described earlier (Han et al. 2009, 2010; Korhonen et al. 2010a,b; Turunen et al. 2012); thus, only a brief account is given here. First, image stacks were imported into ImageJ (National Institute of Health, USA) and 8–10 living cells (confirmed with bright fluorescence and the absence of propidium iodide staining that was used to reveal dead cells) from each sample at each time point were chosen for analysis. The analyzed cells were located at a depth of approximately 20–40 μm from the cartilage surface (Fig. 2a). To detect the edges of cells and to determine cell volumes, a threshold was determined by imaging polystyrene fluorescent microspheres (Polyscience Europe GmbH, Eppelhelm) of 7.32 μm in diameter (volume 205.4 μm^3). A threshold of 40 % of the maximum fluorescence intensity gave correct volumes for the microspheres (volume 206.4 μm^3) and thus was chosen as the threshold for cell volume analysis. The same threshold and a similar calibration technique have been used previously (Bush and Hall 2001a,b, 2003, 2005; Turunen et al. 2012). The Visualization Toolkit 5.2.0 (Kitware, Inc.) was used for reconstructing 3D images of the cells (Fig. 2a), and a code programmed with Python was used for calculating cell volumes (for more details, see Alyassin et al. (1994)). For the analysis of width, depth, and height of cells, *x*- and *y*-directions in the horizontal plane were defined along the minor and major axes of the cell cross-sections that were perpendicular to the *z*-direction (height of cells). Width, depth, and height were then determined by analyzing maximum distances between cell edges in *x*-, *y*-, and *z*-directions, respectively, using MAT-

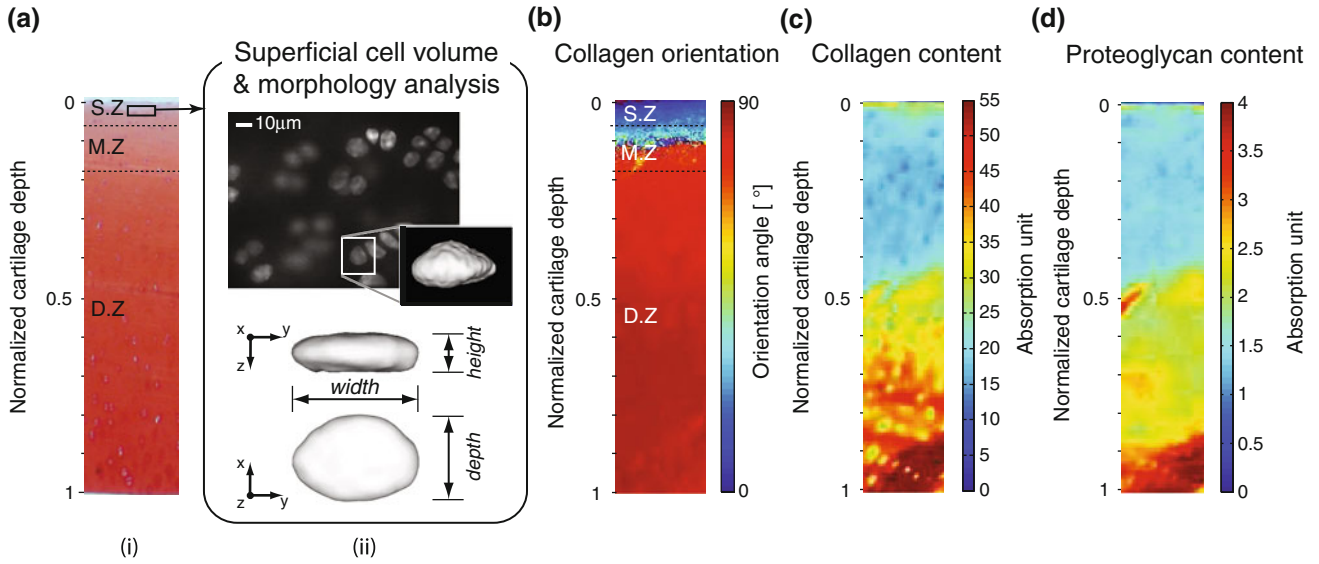

Fig. 2 **a** A light microscopy image illustrating the location of analyzed cells (zone thicknesses were approximated from PLM, *S.Z* = superficial zone, *M.Z* = middle zone, and *D.Z* = deep zone) (*i*) and a typical confocal microscopy image of the calcein-AM-stained cells with a 3D presentation of a chondrocyte, including definition of cell dimensions (*ii*). Typical PLM (**b**) and FTIR images (**c**, **d**) for the determination of collagen orientation and collagen and PG content, respectively, are also shown

LAB R2007b (MathWorks Inc., USA) (Han et al. 2009, 2010; Turunen et al. 2012).

2.4 Polarized light microscopy (PLM)

In order to reveal changes in the collagen orientation of the samples as a result of collagenase treatment, PLM was used (Fig. 2b) (Arokoski et al. 1996; Bennett 1950; Rieppo et al. 2003). Processing of the samples, measurements, and analysis has been described earlier in detail, thus, only a brief description is given here (for specific details, see Kiraly et al. (1997) and Rieppo et al. (2008) and Rieppo et al. (2009)).

First, the frozen samples were thawed. Then, the specimens were fixed in phosphate-buffered 10 % formalin, decalcified, dehydrated, and treated with xylene before embedding in paraffin (Paraplast Plus, Lancer Division of Sherwood Medical, Kildare, Ireland). Three microscopic sections of 5 µm in thickness were prepared from each sample using a microtome (LKB 2218 HistoRange microtome, LKB produkter Ab, Bromma, Sweden) and thereafter deparaffinized and treated with hyaluronidase to remove PGs (1,000 U ml^{-1} hyaluronidase, Sigma-Aldrich). The measurements for unstained microscopic sections were taken using a Leitz Ortholux II POL polarized light microscope (Leitz, Wetzlar, Germany), and a Peltier-cooled, high-performance CCD camera (Photometrics SenSys, Roper Scientific, Tucson, AZ, USA) was used for signal detection. The width of the measurement region was ~400 µm and the length of the region extended from the cartilage surface to the cartilage–bone interface. Analysis of collagen orientation, which has been described in detail in earlier studies (Rieppo et al. 2008, 2009), was based on the Stokes parameters.

2.5 Fourier transform infrared (FTIR) microspectroscopy

To determine collagen and PG contents of intact and degraded cartilage, FTIR microspectroscopy was used (Fig. 2c, d). In FTIR microspectroscopy, absorption of infrared light is measured pixel-by-pixel within a microscopic tissue section, and subsequently, an infrared absorption spectrum is obtained for each pixel. As different molecules in biological samples show different absorption characteristics, it is possible to determine the amount of molecules of interest, that is, PG and collagen in articular cartilage (Bi et al. 2006; Boskey and Camacho 2007; Camacho et al. 2001).

Three unstained, 5-µm-thick sections from each sample were prepared from the frozen samples (after initial thawing, the samples were frozen with liquid nitrogen) with a cryomicrotome (Reichert-Jung Cryostat 2800 Frigocut-E, Nussloch, Germany) and placed on Zinc Selenide (ZnSe) windows for FTIR microspectroscopy. Measurements were taken using a PerkinElmer Spectrum Spotlight 300 FTIR-imaging system (PerkinElmer, Shelton, CO, USA) in transmission mode using the following measurement parameters: spectral resolution = 4 cm^{-1}, pixel size = 6.25 µm, scans per pixel = 2. During the FTIR measurements, the sample box was purged with CO_2-free dried air to standardize the measurement conditions (Parker Balston, Haver-

hill, MA, USA). The width of the measurement region was ~400 μm and the length of the region extended from the surface of the cartilage to the cartilage–bone interface.

Spectra were first corrected for the offset by subtracting the minimum value of the spectra. Subsequently, PG and collagen contents were determined from the integrated absorbance of the carbon region (1,140–985 cm^{-1}) and amide I peak (1,585–1,720 cm^{-1}), respectively (Bi et al. 2006; Boskey and Camacho 2007; Camacho et al. 2001; Saarakkala et al. 2010). Finally, the depth-wise profiles of PG and collagen contents were calculated for each sample by averaging the integrated absorbance values parallel to the surface.

2.6 Biomechanical testing

In order to quantify the biomechanical changes of the samples due to the collagenase treatment, stepwise stress-relaxation tests were conducted for the samples in an unconfined compression geometry using a high-resolution mechanical testing instrument (Töyräs et al. 1999). Prior to the biomechanical measurements, the samples were thawed. The measurement chamber was filled with phosphate-buffered saline (PBS, isotonic osmolarity) and the metallic compression plate was driven to the bottom of the testing chamber. This was set as the offset position. The compression plate was then elevated and the sample was set under the plate. An initial contact between the sample surface and metallic plate was sensitively observed from a change in the force sensor reading. Then, the compression plate was further driven slowly to obtain a full contact between the cartilage surface and metallic plate. The full contact was confirmed visually by ensuring that no light could be seen through the sample surface–metallic plate interface. Thickness of the samples (1.1 ± 0.3 mm and 1.2 ± 0.3 mm for intact and degraded cartilage, respectively) was defined at full contact.

Stepwise stress-relaxation tests were conducted for the samples ($2 \times 5\,\%$ strain, 30 min relaxation after each step, 2 mm s^{-1} loading velocity, that is, $189 \pm 52\,\%\ s^{-1}$ strain rate) (Fig. 3). Two steps were applied to characterize the nonlinearity of the samples. Based on earlier studies, 30 min relaxation was assumed to be enough to reach equilibrium conditions (Jurvelin et al. 1997; Korhonen et al. 2003). As changes in the collagen fibril network, caused by the collagenase treatment, change the peak forces in the stress-relaxation experiments (Korhonen et al. 2003), the loading velocity was the maximum velocity possible with the equipment. Instantaneous and equilibrium moduli of the samples were calculated as a stress–strain ratio from the peak and equilibrium forces of the stress-relaxation curves (Fig. 3), respectively, both at 5 and 10 % strains for the intact and degraded cartilage samples.

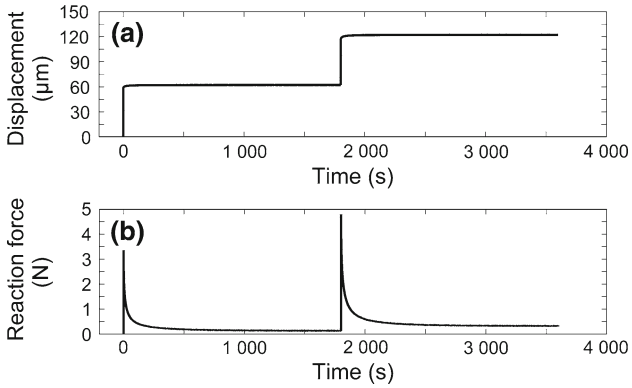

Fig. 3 A schematic presentation of the stress-relaxation protocol: **a** displacement and **b** reaction force as a function of time

2.7 Statistical analysis

All results are presented as means ± standard deviations (SD). From each joint (7 joints in total), two samples were prepared; one was degraded with collagenase ($n = 7$) and the intact sample served as a control sample ($n = 7$) (Fig. 1). The number of samples for both groups (intact and degraded cartilage) is given as n and the number of cells analyzed as N. A mixed linear model with Sidak correction was used for comparing cell volume and shape between the control and digested samples (Brown and Prescott 2006). In the model, the time of measurement, type of sample, and their interaction were set as fixed variables, while the sample number was taken as the random variable. The same statistical test has been applied earlier for similar comparisons (Korhonen et al. 2011; Saarakkala et al. 2010; Turunen et al. 2012). In order to compare collagen content, PG content, collagen orientation, and biomechanical properties (equilibrium and instantaneous modulus) between the control and digested samples, the nonparametric Wilcoxon signed rank test was used. A nonparametric test was chosen because the number of samples was small and the data were not normally distributed (Shapiro–Wilk test). All statistical analyses were performed with SPSS 17.0 (Chicago, IL, USA).

3 Results

3.1 Confocal laser scanning microscopy (CLSM)

In the intact cartilage samples, volume and height of the cells at 20 min following the hypotonic challenge were significantly greater than those before the challenge (Table 2). After this time point, volume and height of the cells decreased significantly, but volume did not regain its original value (Table 2). In contrast, volume and height of cells in the degraded cartilage samples had recovered back to the origi-

Table 2 Cell volume, height, width, depth, and aspect ratios before the hypotonic loading (resting values) and 20 and 120 min after the loading in intact and degraded cartilage samples. Exactly the same cells were not analyzed at each time point

Cell morphological parameter (N = 55–64/time point)		Intact cartilage Mean ± SD (n = 7)	Degraded cartilage Mean ± SD (n = 7)
Volume (μm^3)	Resting value	265 ± 83	289 ± 88
	20 min after loading	338 ± 113*	287 ± 104
	120 min after loading	294 ± 65*,***	283 ± 65
Height (μm)	Resting value	4.3 ± 1.1	4.7 ± 1.2
	20 min after loading	5.2 ± 1.2*	4.5 ± 1.4
	120 min after loading	4.6 ± 1.0**	4.6 ± 1.0
Width (μm)	Resting value	12.2 ± 2.5	11.8 ± 1.5
	20 min after loading	12.1 ± 1.9	12.4 ± 2.0
	120 min after loading	12.4 ± 1.9	11.5 ± 1.8*
Depth (μm)	Resting value	9.1 ± 1.7	9.1 ± 1.3
	20 min after loading	9.3 ± 1.4	8.9 ± 1.2
	120 min after loading	9.4 ± 1.3	9.2 ± 1.3
Aspect ratio (height/width)	Resting value	0.37 ± 0.14	0.41 ± 0.13
	20 min after loading	0.44 ± 0.13	0.38 ± 0.13
	120 min after loading	0.38 ± 0.11	0.42 ± 0.13
Aspect ratio (height/depth)	Resting value	0.49 ± 0.16	0.53 ± 0.16
	20 min after loading	0.57 ± 0.14	0.52 ± 0.17
	120 min after loading	0.49 ± 0.12	0.51 ± 0.14

* $p < 0.05$ and ** $p < 0.01$, as compared to previous time point
*** $p < 0.05$, as compared to the resting value

nal values and were the same before and at 20 and 120 min after the osmotic challenge (Table 2). From 20 to 120 min after the hypotonic challenge, cell width changed significantly in the degraded cartilage samples, while it remained the same in the intact group (Table 2). In both groups, cell depth and aspect ratios were unaltered relative to the original values at the steady-state time points following the osmotic challenge (Table 2).

Normalized cell volume and height at 20 min following the hypotonic loading were significantly smaller in the degraded compared to the intact cartilage (Figs. 4a, b). Normalized cell volume remained significantly smaller in the degraded cartilage also at 120 min following the hypotonic loading. Normalized cell width was significantly greater in the degraded compared to the intact cartilage samples at the 20 min time point. Normalized cell depth was similar in both groups.

3.2 Polarized light microscopy (PLM)

Twenty-four hours of collagenase treatment increased the orientation angle of the collagen fibrils in the top ~10 % of the cartilage significantly (n = 7 per group, $p < 0.05$, Fig. 5), that is, the orientation angle was more perpendicular to the surface in the degraded (42° ± 15°, mean within the top 10 % of the cartilage) than the intact cartilage (32° ± 10°). Deeper zones did not experience changes in the collagen orientation as a result of the collagenase treatment.

3.3 Fourier transform infrared (FTIR) microspectroscopy

Collagenase treatment for 24 h reduced the collagen content in the top ~10 % of the cartilage significantly (n = 7 per group, $p < 0.05$, Fig. 6). The PG content remained unaffected by the collagenase treatment in the same zone (n = 7 per group, $p > 0.05$, Fig. 7). In the deeper zones, neither collagen nor PG content was different between the intact and enzymatically degraded cartilage (n = 7 per group, $p > 0.05$).

3.4 Biomechanical testing

The instantaneous modulus, as calculated from the peak forces of the stress-relaxation curves (Fig. 3b), was significantly lower for the degraded compared to the intact cartilage samples at 5 and 10 % strains (n = 7 per group, $p < 0.05$, Table 3). The collagenase treatment did not change the equilibrium modulus of the samples ($p > 0.05$, Table 3).

4 Discussion

Confocal laser scanning microscopy was used to study the effects of long-term hypotonic challenges on cell volume changes in the superficial zone of intact and enzymatically

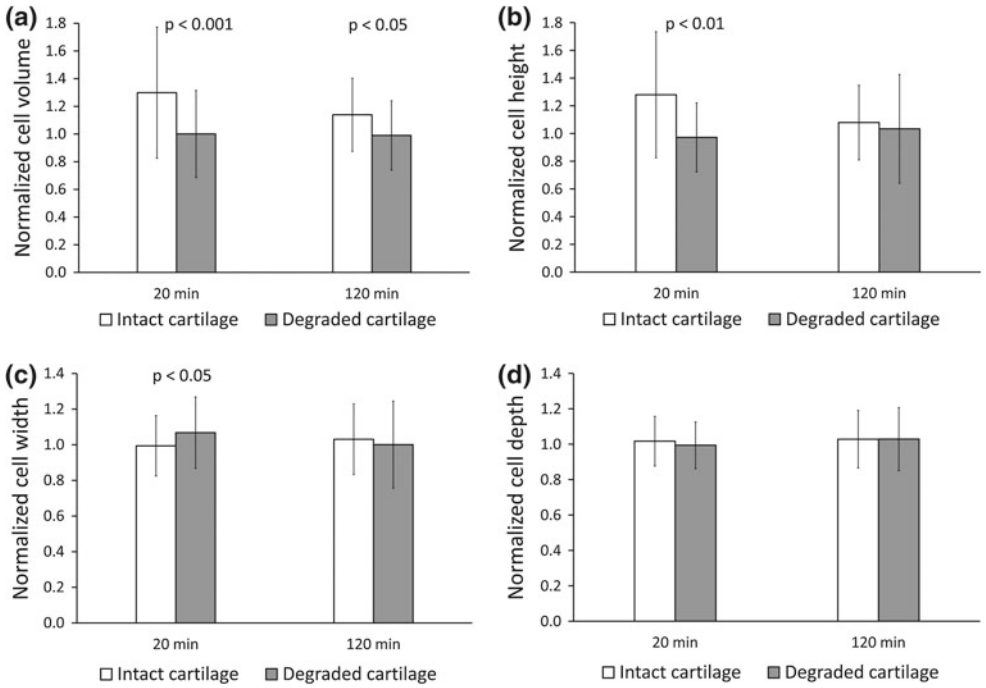

Fig. 4 Normalized cell volume (**a**), height (**b**), width (**c**), and depth (**d**) of the samples at steady state after the hypotonic challenge (cell parameter after the hypotonic challenge divided by the parameter before the osmotic challenge). Data are expressed as mean ± SD

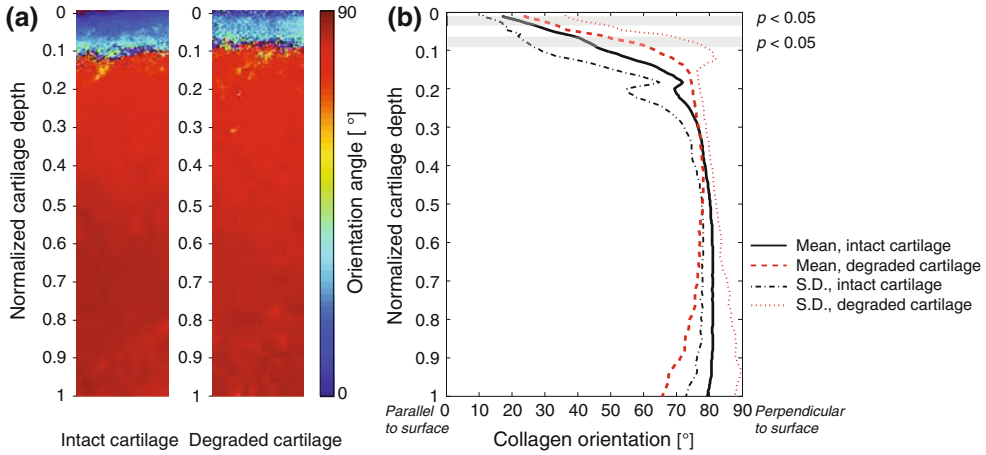

Fig. 5 **a** Typical PLM images of collagen orientation angle and **b** mean collagen orientation angle (°) as a function of normalized depth of the intact and enzymatically degraded samples (0 = cartilage surface and 1 = cartilage–bone interface). Significant difference ($p < 0.05$) between the groups was found in the superficial zone

degraded bovine articular cartilage. Changes in cartilage composition (collagen and PG contents) and collagen orientation due to collagen degradation were quantified with FTIR microspectroscopy and PLM, and biomechanical tests were used to characterize the instantaneous and equilibrium modulus of the samples. As hypothesized, cell volumes 20 and 120 min after the hypotonic challenge relative to those before the challenge (i.e., normalized cell volumes) were significantly greater for the intact cartilage than the degraded cartilage samples. Collagen content decreased significantly in the superficial zone due to the enzymatic treatment, while PG content did not change. The instantaneous modulus was reduced and the collagen fibril orientation angle was increased in the superficial zone as a result of the collagenase treatment. These findings suggest that the collagen network contributes to modulating chondrocyte volume and morphology.

Several previous studies using either intact cartilage, cartilage explants, or isolated cells have shown that cell volumes increase at early (minutes) time points after applying

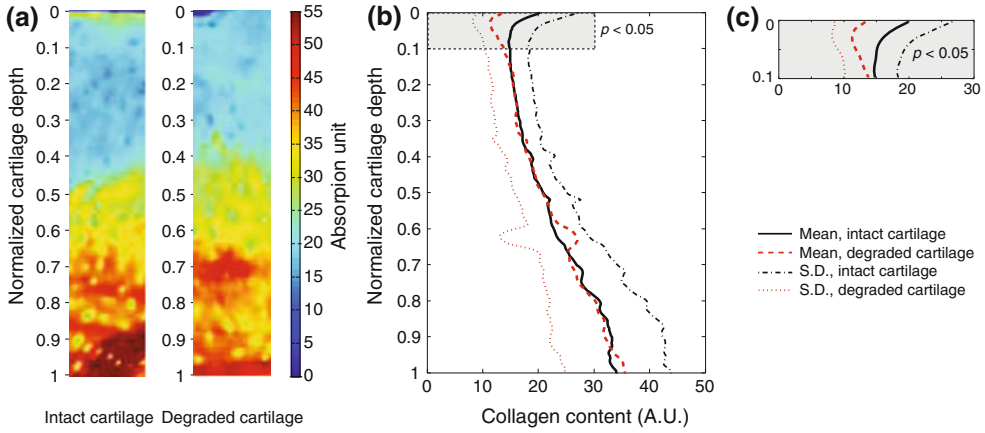

Fig. 6 **a** Typical FTIR microspectroscopy images of collagen content and **b** mean collagen content (A.U. = absorption unit) as a function of normalized depth of the intact and enzymatically degraded samples (0 = cartilage surface and 1 = cartilage–bone interface). A magnification of the superficial zone is also indicated (**c**). Significant difference ($p < 0.05$) between the groups was found in the superficial zone

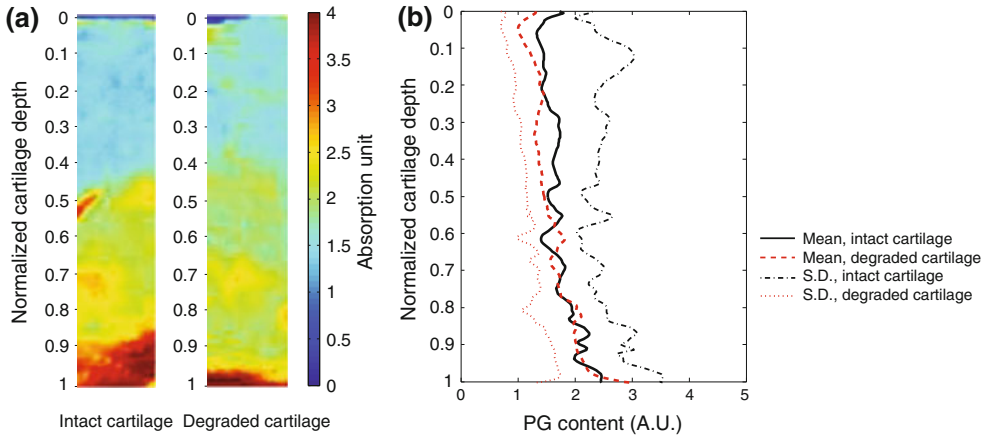

Fig. 7 **a** Typical FTIR microspectroscopy images of PG content and **b** mean PG content (A.U. = absorption unit) as a function of normalized depth of the intact and enzymatically degraded samples (0 = cartilage surface and 1 = cartilage–bone interface)

hypotonic loading (Bush and Hall 2001a; Korhonen et al. 2010b; Turunen et al. 2012). However, differences in the cell volumetric behavior between the aforementioned groups have been suggested to occur after the initial volume increase and, thus, cell volume recovery and long-term cell swelling have been suggested to depend on the surrounding matrix (Korhonen et al. 2010b; Turunen et al. 2012). More specifically, it has been shown that volumes of isolated chondrocytes and chondrocytes in cartilage explants (measurements taken through the cut surface with the ECM compromised) return closely to their initial, pre-intervention values at steady state following a hypotonic challenge (Bush and Hall 2001a; Turunen et al. 2012). In the present study, the behavior of superficial zone cells in degraded cartilage samples (ECM not fully intact) was similar to these former observations. In contrast, superficial zone cells in the intact samples (measurements conducted through the intact cartilage surface, ECM fully intact) did not recover to the original volume, but remained approximately 20 % larger at 20 and 120 min following the hypotonic challenge. This result is consistent with earlier studies conducted on intact cartilage where similar osmotic challenges were used (Korhonen et al. 2010b; Turunen et al. 2012). Cell morphology analysis revealed that cell height was the most dominant factor accounting for the difference between the groups, similarly as in Turunen et al. (2012), while cell width and depth had negligible roles. Due to the continuous swelling of the ECM (Flahiff et al. 2002; Korhonen et al. 2010b; Narmoneva et al. 1999), especially in the axial direction, and physical links between the ECM and the cell membrane (Loeser 2000), cell height and volume recovery may have been partially prevented/delayed in the intact tissue. Also, tissue swelling may have allowed cells to expand to a state in which they did not have a need to regulate their height and volume. This is supported by the similar final absolute cell volume (volume at 120 min time point) in both groups (Table 2).

Table 3 Instantaneous and equilibrium moduli of intact ($n = 7$) and collagenase-treated ($n = 7$) cartilage samples (mean ± SD) at different compressive strains. The instantaneous modulus decreased significantly after collagenase treatment, while no significant change in the equilibrium modulus was noticed

	Intact cartilage	Collagenase treated cartilage
Instantaneous modulus (MPa)		
5 % strain	7.0 ± 6.3 MPa	3.6 ± 3.7 MPa*
10 % strain	10.6 ± 9.3 MPa	5.4 ± 4.6 MPa*
Equilibrium modulus (MPa)		
5 % strain	0.3 ± 0.3 MPa	0.2 ± 0.3 MPa
10 % strain	0.5 ± 0.3 MPa	0.3 ± 0.3 MPa

* $p < 0.05$, as compared to intact cartilage

Resting volumes (i.e., volumes in the isotonic medium of 285 mOsm) of superficial zone chondrocytes found in this study were similar to those found recently in intact articular cartilage; 265 versus 327 μm^3 (Han et al. 2009, rabbit patella), 250 μm^3 (Han et al. 2010, rabbit patella), and 260 μm^3 (Turunen et al. 2012, bovine lateral patellar groove). Other studies reported slightly greater cell volumes (Bush and Hall 2001a,b, bovine metacarpal phalangeal; Bush and Hall 2003, human knee joint; Korhonen et al. 2010a,b, rabbit patella). These differences might be explained by the difference in species (bovine, human, and rabbit), different locations in the joints (lateral patellar groove, metacarpal phalangeal, tibial plateau, and patellae), measurement depths (superficial zone vs. superficial zone + mid zone + deep zone), degeneration of the sample, age differences, exact medium osmolarity (280–300 mOsm), sample preparation (tissue explant vs. intact tissue), and individual differences.

All samples were frozen following the CLSM measurements in PBS (−20 °C) and thawed slowly in a water bath (room temperature) prior to structural and mechanical measurements. Based on earlier studies (Szarko et al. 2010; Changoor et al. 2010), the freezing–thawing method has been suggested to produce no significant effect on the dynamic mechanical properties of cartilage. Based on the studies of Zheng et al. (2009) and Laouar et al. (2007), there might be some loss of GAGs due to freezing. In any case, all of our samples (intact and degraded samples) underwent the same freezing–thawing protocol; therefore, we expected the protocol to have a similar effect on all samples from both groups.

It has been shown previously that collagenase treatment reduces collagen fibril diameter, collagen fibril network stiffness, and collagen fibril organization and quantity in the superficial zone of cartilage (Table 1) (Korhonen et al. 2003; Långsjö et al. 2002; Rieppo et al. 2003). These results are in line with the present findings: collagen content and instantaneous modulus of the cartilage samples were reduced after the collagenase treatment. Consistent with an earlier study (Rieppo et al. 2003), the mean collagen orientation angle was increased as a result of the enzymatic treatment, indicating fibrillation of the superficial collagen fibril network. It is also possible that the mean collagen fibril diameter (Långsjö et al. 2002) and the collagen fibril network stiffness (Korhonen et al. 2003) were reduced following collagenase treatment, as suggested by the reduced collagen content and reduced instantaneous modulus, and these factors may have contributed to the swelling of the superficial zone cartilage. This swelling may have caused a re-organization and re-orientation of the collagen fibrils. Since the normalized steady-state cell volumes following the osmotic loading were altered, and collagen orientation and content, as well as biomechanical properties of the cartilage were altered after the collagenase treatment, the present results, together with earlier studies (Korhonen et al. 2003; Långsjö et al. 2002; Rieppo et al. 2003), suggest that cell volume changes in cartilage are strongly modulated by the collagen fibril network.

The instantaneous cartilage modulus and the collagen fibril network modulus have been shown to be strongly related to collagen content and organization in articular cartilage (Julkunen et al. 2007; Korhonen et al. 2002, 2003). Our results agree with these earlier findings, that is, the instantaneous modulus was reduced significantly as a consequence of the collagenase treatment and was associated with a decrease in the collagen content. Furthermore, there was a strain dependence of the instantaneous modulus, in agreement with earlier findings of strain-dependent increases in peak stiffness and collagen fibril network modulus (Julkunen et al. 2007; Langelier and Buschmann 2003; Li et al. 1999). The equilibrium modulus depends strongly on PG content (Julkunen et al. 2007; Korhonen et al. 2003) and thus was not affected by collagenase treatment, as expected, as FTIR microspectroscopy analysis revealed no change in PG content in the degraded cartilage samples. In this study, we did not use a fibril reinforced biphasic model for the analysis of the stress-relaxation measurements. However, we believe that we arrived at the same conclusions as we would have with the fibril reinforced biphasic model, that is, collagen degradation reduces primarily the dynamic (and the fibril network) modulus, while the equilibrium (and the nonfibrillar matrix) modulus is affected less by collagen degradation (Korhonen et al. 2003; Laasanen et al. 2003).

In the biomechanical measurements, the full contact was ensured visually and the pre-force value in the full contact was not exactly the same for all of the samples. This method was used instead of using a pre-defined force method, because the degraded cartilage samples might have been compressed substantially more than the intact tissue samples for the same pre-stress value. Subsequently, use of the pre-defined force could have led to different actual strains between the groups.

In previous studies, chondrocyte volumes were found to increase in degenerated human cartilage and in experimental osteoarthritis (anterior cruciate ligament (ACL) transection) of New Zealand white rabbits (Bush and Hall 2003, 2005; Han et al. 2010), and cells were shown to become more rounded in advanced stages of OA (Korhonen et al. 2011). Results of the present study agree with these previous findings: cell resting volumes were $10 \pm 0.6\,\%$ greater and cells were $\sim 10\,\%$ rounder in the degraded compared to the intact cartilage samples. However, these differences were not statistically significant. This suggests that minor collagen degradation alone may not contribute significantly to cell resting volume and shape. This result is supported by an earlier study (Korhonen et al. 2011), which showed that the cell aspect ratio in human cartilage was similar in healthy tissue and in the early stages of OA.

Our results suggest that collagen content and orientation, as well as subsequent tissue softening, modulate cell volume and morphology following an osmotic challenge of articular cartilage. This is consistent with earlier experimental and computational studies, where the collagen network and tissue integrity affected chondrocyte morphology and volume changes (Korhonen et al. 2010a,b, 2008; Turunen et al. 2012). However, we showed here for the first time the direct influence of mild collagen degradation on cell volume and morphology. The results obtained here could point to important mechanisms regulating cartilage mechanotransduction in degraded and diseased tissue. Interestingly, in a previous study, PG content was correlated significantly with changes in cell volume after a hypotonic challenge (Turunen et al. 2012). These results, together with earlier findings (e.g., Bader et al. 1981; Korhonen and Jurvelin 2010; Mow et al. 1992; Schmidt et al. 1990; Wilson et al. 2005) highlight the interplay between collagen and PGs in articular cartilage and suggest that the different constituents of the complex ECM and PCM may have combined effects in regulating cell volume and mechanotransduction in articular cartilage.

Acknowledgments Financial support from the Academy of Finland (projects 125415, 140730, 218038, 128117, and 127198); Sigrid Juselius Foundation, Finland; National Graduate School of Musculoskeletal Disorders and Biomaterials; Finnish Cultural Foundation (The North Savo Regional Grand); European Research Council (project 281180); Kuopio University Hospital (EVO, Department of Clinical Physiology and Nuclear Medicine); and the Alberta Heritage Foundation for Medical Research Team Grant on Osteoarthritis (Canada) is acknowledged. Authors want also to thank Ms. Jaana Mäkitalo for assistance in the measurements.

References

Alexopoulos LG, Setton LA, Guilak F (2005) The biomechanical role of the chondrocyte pericellular matrix in articular cartilage. Acta Biomater 1:317–325

Alyassin AM, Lancaster JL, Downs JH III, Fox PT (1994) Evaluation of new algorithms for the interactive measurement of surface area and volume. Med Phys 21:741–752

Arokoski JPA, Hyttinen MM, Lapveteläinen T, Takacs P, Kosztaczky B, Modis L, Kovanen V, Helminen HJ (1996) Decreased birefringence of the superficial zone collagen network in the canine knee (stifle) articular cartilage after long distance running training, detected by quantitative polarised light microscopy. Ann Rheum Dis 55:253–264

Arokoski JPA, Jurvelin JS, Väätäinen U, Helminen HJ (2000) Normal and pathological adaptations of articular cartilage to joint loading. Scand J Med Sci Sports 10:186–198

Bader DL, Kempson GE, Barrett AJ, Webb W (1981) The effects of leucocyte elastase on the mechanical properties of adult human articular cartilage in tension. Biochim Biophys Acta 677:103–108

Bennett HS (1950) Methods applicable to the study of both fresh and fixed materials. Themicroscopical investigation of biological materials with polarized light. In: McClung JR (ed) McClung's handbook of microscopical technique. Paul B Hoeber, New York pp 591–677

Bi X, Yang X, Bostrom MP, Camacho NP (2006) Fourier transform infrared imaging spectroscopy investigations in the pathogenesis and repair of cartilage. Biochim Biophys Acta 1758:934–941

Boskey A, Camacho NP (2007) FT-IR imaging of native and tissue-engineered bone and cartilage. Biomaterials 28:2465–2478

Brown H, Prescott R (2006) Applied mixed models in medicine. Wiley, New York

Buschmann MD, Hunziker EB, Kim Y-J, Grodzinsky AJ (1996) Altered aggregan synthesis correlates with cell and nucleus structure in statically compressed cartilage. J Cell Sci 109:499–508

Bush PG, Hall AC (2001a) Regulatory volume decrease (RVD) by isolated and in situ bovine articular chondrocytes. J Cell Physiol 187:304–314

Bush PG, Hall AC (2001b) The osmotic sensitivity of isolated and in situ bovine articular chondrocytes. J Orthop Res 19:768–778

Bush PG, Hall AC (2003) The volume and morphology of chondrocytes within non-degenerate and degenerate human articular cartilage. Osteoarthr Cartil 11:242–251

Bush PG, Hall AC (2005) Passive osmotic properties of in situ human articular chondrocytes within non-degenerate and degenerate cartilage. J Cell Physiol 204:309–319

Camacho NP, West P, Torzilli PA, Mendelsohn R (2001) FTIR microscopic imaging of collagen and proteoglycan in bovine cartilage. Biopolymers 62:1–8

Changoor A, Fereydoonzad L, Yaroshinsky A, Buschmann MD (2010) Effects of refrigeration and freezing on the electromechanical and biomechanical properties of articular cartilage. J Biomech Eng 132:064502

Flahiff C, Narmoneva D, Huebner J, Kraus V, Guilak F, Setton L (2002) Osmotic loading to determine the intrinsic material properties of guinea pig knee cartilage. J Biomech 35:1285–1290

Grushko G, Schneiderman R, Maroudas A (1989) Some biochemical and biophysical parameters for the study of the pathogenesis of osteoarthritis: a comparison between the processes of ageing and degeneration in human hip cartilage. Connect Tissue Res 19:149–176

Guilak F (2011) Biomechanical factors in osteoarthritis. Best Pract Res Clin Rheumatol 25:815–823

Guilak F, Alexopoulos LG, Upton ML, Youn I, Choi JB, Cao LI, Setton LA, Haider MA (2006) The pericellular matrix as a transducer of biomechanical and biochemical signals in articular cartilage. Ann NY Acad Sci 1068:498–512

Han SK, Colarusso P, Herzog W (2009) Confocal microscopy indentation system for studying in situ chondrocyte mechanics. Med Eng Phys 31:1038–1042

Han SK, Seerattan R, Herzog W (2010) Mechanical loading of in situ chondrocytes in lapine retropatellar cartilage after anterior cruciate ligament transection. J R Soc Interface 7:895–903

Hing WA, Sherwin AF, Ross JM, Poole CA (2002) The influence of the pericellular microenvironment on the chondrocyte response to osmotic challenge. Osteoarthr Cartil 10:297–307

Julkunen P, Kiviranta P, Wilson W, Jurvelin JS, Korhonen RK (2007) Characterization of articular cartilage by combining microscopic analysis with a fibril-reinforced finite-element model. J Biomech 40:1862–1870

Jurvelin JS, Buschmann MD, Hunziker EB (1997) Optical and mechanical determination of Poisson's ratio of adult bovine humeral articular cartilage. J Biomech 30:235–241

Kikuchi T, Sakuta T, Yamaguchi T (1998) Intra-articular injection of collagenase induces experimental osteoarthritis in mature rabbits. Osteoarthr Cartil 6:177–186

Kiraly K, Hyttinen MM, Lapveteläinen T, Elo M, Kiviranta I, Dobai J, Modis L, Helminen HJ, Arokoski JP (1997) Specimen preparation and quantification of collagen birefringence in unstained sections of articular cartilage using image analysis and polarizing light microscopy. Histochem J 29:317–327

Korhonen RK, Han SK, Herzog W (2010a) Osmotic loading of articular cartilage modulates cell deformations along primary collagen fibril directions. J Biomech 43:783–787

Korhonen RK, Han SK, Herzog W (2010b) Osmotic loading of in situ chondrocytes in their native environment. Mol Cell Biomech 7:125–134

Korhonen RK, Julkunen P, Jurvelin JS, Saarakkala S (2011) Structural and compositional changes in peri- and extracellular matrix of osteoarthritic cartilage modulate chondrocyte morphology. Cell Mol Bioeng 4:484–494

Korhonen RK, Julkunen P, Wilson W, Herzog W (2008) Importance of collagen orientation and depth-dependent fixed charge densities of cartilage on mechanical behavior of chondrocytes. J Biomech Eng 130:021003

Korhonen RK, Jurvelin JS (2010) Compressive and tensile properties of articular cartilage in axial loading are modulated differently by osmotic environment. Med Eng Phys 32:155–160

Korhonen RK, Laasanen MS, Töyräs J, Lappalainen R, Helminen HJ, Jurvelin JS (2003) Fibril reinforced poroelastic model predicts specifically mechanical behavior of normal, proteoglycan depleted and collagen degraded articular cartilage. J Biomech 36:1373–1379

Korhonen RK, Wong M, Arokoski J, Lindgren R, Helminen HJ, Hunziker EB, Jurvelin JS (2002) Importance of the superficial tissue layer for the indentation stiffness of articular cartilage. Med Eng Phys 24:99–108

Laasanen MS, Töyräs J, Korhonen RK, Rieppo J, Saarakkala S, Nieminen MT, Hirvonen J, Jurvelin JS (2003) Biomechanical properties of knee articular cartilage. Biorheology 40:133–140

Langelier E, Buschmann MD (2003) Increasing strain and strain rate strengthen transient stiffness but weaken the response to subsequent compression for articular cartilage in unconfined compression. J Biomech 36:853–859

Laouar L, Fishbein K, McGann LE, Horton WE, Spencer RG, Jomha NM (2007) Cryopreservation of porcine articular cartilage: MRI and biochemical results after different freezing protocols. Cryobiology 54:36–43

Långsjö TK, Rieppo J, Pelttari A, Oksala N, Kovanen V, Helminen HJ (2002) Collagenase-induced changes in articular cartilage as detected by electron-microscopic stereology, quantitative polarized light microscopy and biochemical assays. Cells Tissues Organs 172:265–275

Li LP, Soulhat J, Buschmann MD, Shirazi-Adl A (1999) Nonlinear analysis of cartilage in unconfined ramp compression using a fibril reinforced poroelastic model. Clin Biomech 14:673–682

Loeser RF (2000) Chondrocyte integrin expression and function. Biorheology 37:109–116

Lyyra T, Arokoski JPA, Oksala N, Vihko A, Hyttinen M, Jurvelin JS, Kiviranta I (1999) Experimental validation of arthroscopic cartilage stiffness measurement using enzymatically degraded cartilage samples. Phys Med Biol 44:525–535

Mankin HJ, Mow VC, Buckwalter JA, Iannotti JP, Ratcliffe A (1994) Form and function of articular cartilage. In: Sheldon RS (ed) Orthopaedic basic science. American Academy of Orthopaedic Surgeons, USA pp 1–44

Maroudas A, Venn M (1977) Chemical composition and swelling of normal and osteoarthrotic femoral head cartilage. II. Swelling. Ann Rheum Dis 36:399–406

Millward-Sadler SJ, Salter DM (2004) Integrin-dependent signal cascades in chondrocyte mechanotransduction. Ann Biomed Eng 32:435–446

Mow VC, Ratcliffe A, Poole AR (1992) Cartilage and diarthrodial joints as paradigms for hierarchical materials and structures. Biomaterials 13:67–97

Narmoneva DA, Wang JY, Setton LA (1999) Nonuniform swelling-induced residual strains in articular cartilage. J Biomech 32:401–408

Newman P, Watt F (1988) Influence of cytochalasin D-induced changes in cell shape on proteoglycan synthesis by cultured articular chondrocytes. Exp Cell Res 178:199–210

Nieminen MT, Töyräs J, Rieppo J, Hakumäki JM, Silvennoinen J, Helminen HJ, Jurvelin JS (2000) Quantitative MR microscopy of enzymatically degraded articular cartilage. Magn Reson Med 43:676–681

Poole CA (1997) Articular cartilage chondrons: form, function and failure. J Anat 191:1–13

Poole CA, Ayad S, Gilbert RT (1992) Chondrons from articular cartilage. V. Immunohistochemical evaluation of type VI collagen organisation in isolated chondrons by light, confocal and electron microscopy. J Cell Sci 103:1101–1110

Poole CA, Flint MH, Beaumont BW (1988) Chondrons extracted from canine tibial cartilage: preliminary report on their isolation and structure. J Orthop Res 6:408–419

Rieppo J, Hallikainen J, Jurvelin JS, Kiviranta I, Helminen HJ, Hyttinen MM (2008) Practical considerations in the use of polarized light microscopy in the analysis of the collagen network in articular cartilage. Microsc Res Tech 71:279–287

Rieppo J, Hyttinen MM, Halmesmäki E, Ruotsalainen H, Vasara A, Kiviranta I, Jurvelin JS, Helminen HJ (2009) Changes in spatial collagen content and collagen network architecture in porcine articular cartilage during growth and maturation. Osteoarthr Cartil 17:448–455

Rieppo J, Töyräs J, Nieminen MT, Kovanen V, Hyttinen MM, Korhonen RK, Jurvelin JS, Helminen HJ (2003) Structure-function relationships in enzymatically modified articular cartilage. Cells Tissues Organs 175:121–132

Saarakkala S, Julkunen P, Kiviranta P, Mäkitalo J, Jurvelin JS, Korhonen RK (2010) Depth-wise progression of osteoarthritis in human articular cartilage: investigation of composition, structure and biomechanics. Osteoarthr Cartil 18:73–81

Schmidt MB, Mow VC, Chun LE, Eyre DR (1990) Effects of proteoglycan extraction on the tensile behavior of articular cartilage. J Orthop Res 8:353–363

Stockwell RA (1991) Cartilage failure in osteoarthritis: relevance of normal structure and function. Rev Clin Anat 4:161–191

Stockwell RA, Meachim G (1973) The chondrocytes. In: Freeman MAR (ed) Adult articular cartilage. Alden Press, Oxford pp 51–99

Szarko M, Muldrew K, Bertram JEA (2010) Freeze-thaw treatment effects on the dynamic mechanical properties of articular cartilage. BMC Musculoskel Disord 11:231

Töyräs J, Rieppo J, Nieminen MT, Helminen HJ, Jurvelin JS (1999) Characterization of enzymatically induced degradation of articular cartilage using high frequency ultrasound. Phys Med Biol 44:2723–2733

Turunen SM, Lammi MJ, Saarakkala S, Koistinen A, Korhonen RK (2012) Hypotonic challenge modulates cell volumes differently in the superficial zone of intact articular cartilage and cartilage explant. Biomech Mod Mechanobiol 11:665–675

Urban JP, Hall AC, Gehl KA (1993) Regulation of matrix synthesis rates by the ionic and osmotic environment of articular chondrocytes. J Cell Physiol 154:262–270

Wilson W, Van Donkelaar CC, Van Rietbergen B, Huiskes R (2005) A fibril-reinforced poroviscoelastic swelling model for articular cartilage. J Biomech 38:1195–1204

Zheng S, Xia Y, Bidthanapally A, Badar F, Ilsar I, Duvoisin N (2009) Damages to the extracellular matrix in articular cartilage due to cryopreservation by microscopic magnetic resonance imaging and biochemistry. Magn Reson Imaging 27:648–655